Pablo R. Brito-Parada[1,*]
Ruben Markus Dewes[2]
Dennis Vega-Garcia[1]
Jan J. Cilliers[1]

Influence of Design Parameters on Biomass Separation in Mini-hydrocyclones

Small hydrocyclones are an attractive technology for biomass separation from fermentation processes. The interactive effect of design parameters on the performance of mini-hydrocyclones is, however, not fully explored and studies are often limited by the challenges in manufacturing such small units. Here, 10-mm mini-hydrocyclones are produced by 3D printing and the impact of spigot diameter, vortex finder diameter and height on separation performance is studied. A central composite rotatable design was adopted to obtain information on the relation between the variables and their influence on concentration ratio and recovery of yeast from a highly diluted system. A Pareto front for separation performance was generated and shown to be suitable to select an optimal design for a set of process constraints.

Keywords: Biomass separation, 3D printing, Mini-hydrocyclones, Yeast

Received: June 07, 2018; *revised:* August 15, 2018; *accepted:* August 30, 2018

DOI: 10.1002/ceat.201800290

1 Introduction

The downstream processing of fermentation products from renewable feedstocks is complex and expensive, which currently hinders their competitiveness levels. The bioproducts of interest are often present in highly diluted aqueous systems that need to be concentrated. A first step in the separation and purification of such systems is the separation of biomass, which is usually achieved by filtration, centrifugation, or sedimentation. However, the efficacy of filters can be limited due to low capacity and high maintenance costs, centrifuges often require high maintenance and investment costs [1], and sedimentation suffers from long residence times [2].

In hydrocyclones, the cut size that can be achieved is directly proportional to their diameter, so mini-hydrocyclones, e.g., 10 mm in diameter, offer an attractive alternative for bioseparations. The residence time in mini-hydrocyclones is short, their maintenance is easy, and they can be applied to continuous processes; in addition, these units do not contain moving parts and can be easily sterilized.

Many studies have focused on the effect of operating parameters on the concentration of yeast biomass from diluted systems using mini-hydrocyclones. It has been shown that separation efficiency can be increased by operating at higher flow rates [3] and also at lower yeast feed concentrations [3–6]. Separation can also be enhanced at higher operating pressures [4, 5, 7] and at higher temperature [4].

Design aspects of mini-hydrocyclones for the concentration of yeast have also received attention in the literature, either comparing different commercial units [4, 8] or assessing geometrical design parameters. In general, it is well understood that the concentration ratio increases with vortex finder diameter and decreases with spigot diameters [4]. Bicalho et al. [7] found that the separation efficiency of yeast in a 10-mm hydrocyclone was increased by reducing the inlet and vortex finder diameters as well as the angle of the conical section, although without neither varying the spigot diameter nor the height of the vortex finder.

The height of the vortex finder has been found to have an impact on the tangential velocities between the conical and cylindrical sections of mini-hydrocyclones [9], with the deeper inserts resulting in lower tangential velocities. Hwang and Chou [10], on the other hand, assessed different vortex finder structures in mini-hydrocyclones and evaluated the effects of their thickness, height, and shape on particle separation efficiency.

Despite multiple studies on the influence of design on mini-hydrocyclone performance, multiple levels for the variables of interest and the investigation of nonlinear trends and interactive effects have not been fully explored. A limitation in the studies of design variables in mini-hydrocyclones might be linked to the difficulties in manufacturing these units, which are often made of acrylic materials. The 3D printing technology can provide the resolution required to accurately manufacture mini-hydrocyclones and has been used recently to manufacture novel designs [11, 12].

In this work, the effect of vortex finder diameter, spigot diameter, and vortex finder height on the separation efficiency

[1]Dr. Pablo R. Brito-Parada, Dennis Vega-Garcia, Prof. Jan J. Cilliers
p.brito-parada@imperial.ac.uk
Imperial College London, Department of Earth Science and Engineering, South Kensington Campus, SW7 2AZ London, UK.
[2]Ruben Markus Dewes
University of Kaiserslautern, Erwin-Schrödinger-Strasse 44, 67663 Kaiserslautern, Germany.

of yeast in 10-mm mini-hydrocyclones is investigated. Multiple mini-hydrocyclone designs were 3D-printed and used in a central composite rotatable design (CCRD) [13] set of experiments to understand the interactions between the aforementioned design variables and generate predictive models and response surfaces of the separation performance.

2 Experimental Setup

The mini-hydrocyclones used in this work were 3D-printed on transparent acrylic (VeroClear) using an Objet30 Pro printer, which has a horizontal build layer of 28 µm and a build resolution of 600×600×900 dpi. All the designs were 10 mm in diameter, 51.4 mm in height, and with a tangential inlet of 4 mm^2. Three factors were varied: the vortex finder diameter (*VF*[1)]), the spigot diameter (*SP*), and the vortex finder height (*VF-H*).

A CCRD experiment considering these three factors was conducted to determine the influence of design parameters on the separation performance of the mini-hydrocyclones, i.e., recovery and concentration ratio. The center point for the experimental design had a *VF* of 2.5 mm, *SP* of 2.5 mm, and *VF-H* of 5 mm. The other points used in the CCRD experiments, which were run in a randomized order, are presented in Tab. 1.

Table 1. Details of the CCRD experimental design with values for vortex finder diameter (*VF*), spigot diameter (*SP*), and vortex finder height (*VF-H*).

VF [mm]	*SP* [mm]	*VF-H* [mm]
2.5	2.5	5
1.5	2.5	5
3.5	2.5	5
2.5	1.5	5
2.5	3.5	5
2.5	2.5	8
2.5	2.5	2
1.9	1.9	3.2
1.9	1.9	6.8
3.1	1.9	3.2
3.1	1.9	6.8
1.9	3.1	3.2
1.9	3.1	6.8
3.1	3.1	3.2
3.1	3.1	6.8

For the experiments, the mini-hydrocyclone units were placed in a housing located above a sump tank, which had a stirrer to maintain the particles suspended. The overflow and underflow discharged into the sump and enabled the collection of samples for analysis. A diluted suspension of yeast, *Saccharomyces cerevisiae*, with a concentration of 0.5 g L^{-1}, was selected. The density of the yeast was 1100 kg m^{-3}. A Malvern Mastersizer 2000 was used to carry out measurements of the particle size distribution of the yeast cells, as indicated in Tab. 2.

Table 2. Particle size distribution of yeast cells used in the experiments.

Parameter	Value
d_{10} [µm]	3.677
d_{20} [µm]	4.111
d_{50} [µm]	5.126
d_{80} [µm]	6.383
d_{90} [µm]	7.124

The feed flow rate to the hydrocyclones was set to 65 mL s^{-1}. It is relevant to point out that the designs that had both *VF* and *SP* of 1.9 mm, exhibited higher pressure requirements and were close to the limits in operating range of the experimental rig. Samples of the overflow and underflow streams were taken to determine the volumetric flow rates. The concentration of yeast on these streams was measured by a Laxco DSM cell density meter.

To assess whether yeast cell breakage takes place, trypan blue exclusion was conducted for samples of the underflow for three different designs. For this purpose, a solution of 0.5 mL of 0.4 % trypan blue was mixed with 0.5 mL of the yeast suspension from the underflow samples, and after 15 min, the solution was added into a Bright-Line hemacytometer (Hausser Scientific), where cell counting was performed. The exclusion was conducted for the center point hydrocyclone and a hydrocyclone with *SP* = 1.9 mm, *VF* = 1.9 mm, and *VF-H* = 3.2 mm, as for the latter the highest shear stress is expected. The viability loss of yeast cells for these designs was 2.9 and 2.3 %, respectively.

3 Results and Discussion

The average underflow and overflow flow rates for all the mini-hydrocyclone designs tested as part of the CCRD experiments carried out are summarized in Tab. 3. The standard deviations for the flow rate measurements were between 0.03 and 0.79 mL s^{-1}. The concentration of yeast for each stream is also presented in Tab. 3.

1) List of symbols at the end of the paper.

Table 3. Average underflow and overflow flow rates and corresponding yeast concentrations for all the mini-hydrocyclone designs tested as part of the CCRD experiments.

Vortex finder diameter [mm]	Spigot diameter [mm]	Vortex finder height [mm]	Flow rates		Concentrations	
			Underflow [mL s^{-1}]	Overflow [mL s^{-1}]	Underflow [g L^{-1}]	Overflow [g L^{-1}]
2.5	2.5	5	36.03	28.72	0.67	0.29
1.5	2.5	5	57.57	7.11	0.51	0.45
3.5	2.5	5	17.19	46.83	0.62	0.45
2.5	1.5	5	9.59	55.39	0.94	0.42
2.5	3.5	5	54.21	10.27	0.52	0.39
2.5	2.5	8	36.28	28.60	0.65	0.31
2.5	2.5	2	38.72	25.79	0.70	0.21
1.9	1.9	3.2	32.42	23.17	0.73	0.18
1.9	1.9	6.8	32.61	24.01	0.70	0.23
3.1	1.9	3.2	12.18	52.14	0.70	0.45
3.1	1.9	6.8	10.37	54.28	0.71	0.46
1.9	3.1	3.2	60.97	4.31	0.50	0.47
1.9	3.1	6.8	57.57	6.48	0.50	0.48
3.1	3.1	3.2	38.70	25.58	0.63	0.31
3.1	3.1	6.8	35.96	28.08	0.62	0.35

3.1 Recovery of Solids

The recovery of solids from the experiments can be calculated as the ratio of the mass flow rate of particles (yeast) in the underflow, $m_{\text{yeast,UF}}$, to the mass flow rate of particles in the feed, $m_{\text{yeast,Feed}}$ (Eq. (1)):

$$R = \frac{m_{\text{yeast,UF}}}{m_{\text{yeast,Feed}}} \times 100\% \quad (1)$$

Contour diagrams of solids recovery are presented in Figs. 1–3. Each figure illustrates the solids recovery as a function of two of the design variables and at different levels of the third one. The recovery of yeast is shown to be affected by all three parameters, with the diameters of both vortex finder and spigot having a larger effect than the vortex finder height.

The contours demonstrate that lower values of vortex finder height result in higher yeast recoveries. It is postulated that for this system the detrimental effect of the vortex finder height is related to the vortex finder obstructing the flow and reducing the percentage of solids reporting to the underflow. The effect of changes in the diameters of the spigot and the vortex finder proved to be more complex. Although in general it would seem that higher recovery values are achieved at lower vortex finder diameters, this is not the case at the higher values of spigot diameters considered in the experiments, where the effect is nonlinear. The nonlinear effect of vortex finder on recovery of yeast is evident.

A regression analysis of the experimental data was then performed to obtain a predictive model for recovery that includes interaction between the variables and up to second-order terms. Eq. (2) describes the mathematical model derived for recovery, R. Note that the regression coefficients for the variables are omitted for clarity (can be found in Tab. 4), and that predictors with p values greater than 0.05 were removed from the model. The model fitness is indicated by a coefficient of determination $R^2 = 0.988$.

Table 4. Regression coefficients for the solids recovery model. Values for the statistically significant design variables (p value < 0.05) are presented; $R^2 = 0.988$.

	Regression coefficient
Intercept	57.971
VF	–25.955
SP	51.985
VF-H	–1.4315
VF/SP	26.515
VF^2	–14.18
SP^2	–18.374

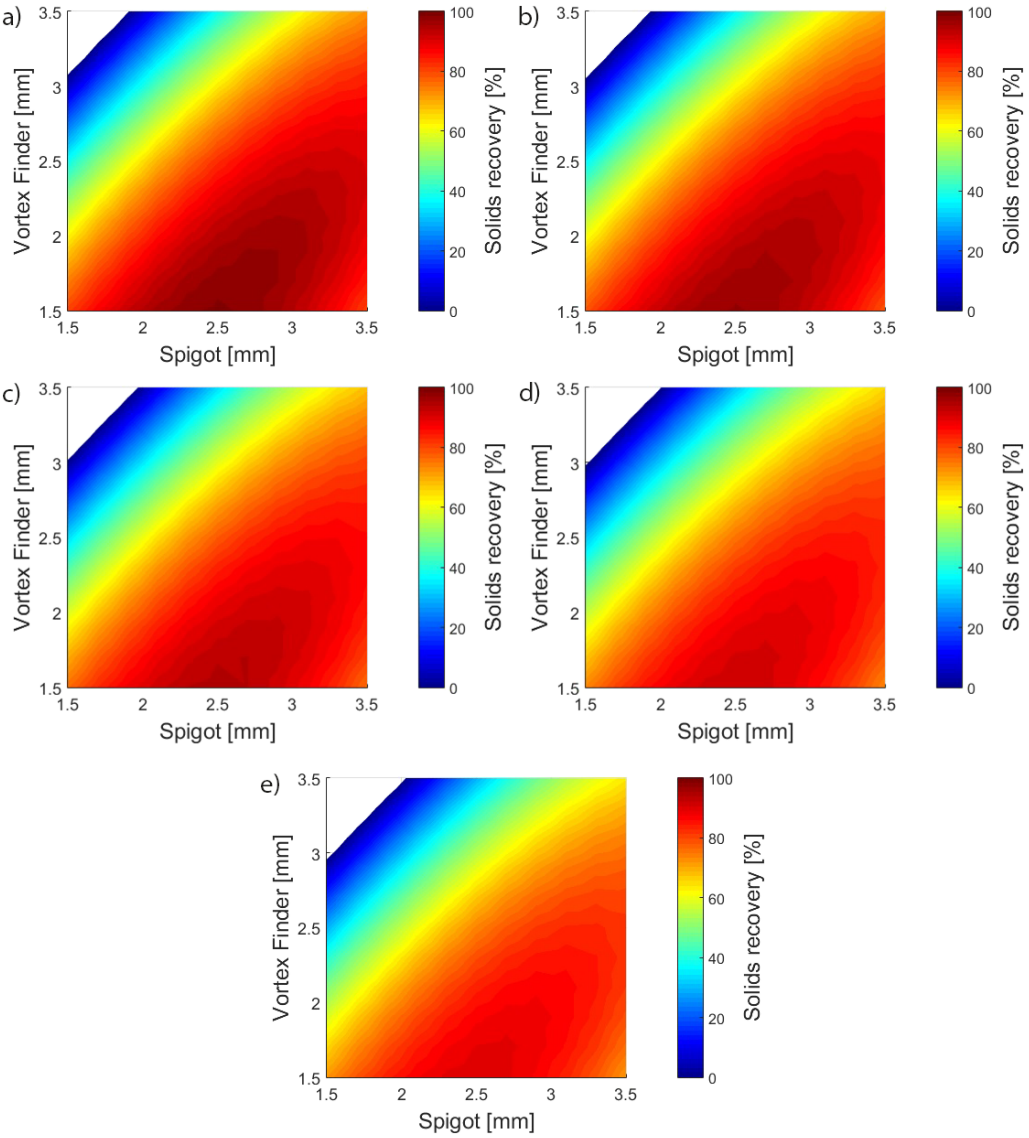

Figure 1. Contour diagrams of solids recovery as a function of vortex finder and spigot diameters for different vortex finder heights: (a) 2 mm, (b) 3.2 mm, (c) 5 mm, (d) 6.8 mm, (e) 8 mm.

$$R = 1 + VF + SP + VF - H + VF\,SP + VF^2 + SP^2 \quad (2)$$

Selecting a mini-hydrocyclone design for a given separation would depend not only on the recovery than can be achieved but also on constraints imposed by the requirements of the process in terms of the concentration ratio. Experimental results for concentration ratio and its modeling are discussed below.

3.2 Concentration Ratio

The concentration ratio, *CR*, is an indication of how many times the percentage of solids in the concentrate is upgraded with regards to that in the feed. For the experiments in this work it is calculated as the ratio between the concentration of yeast in the underflow, $c_{\text{yeast,UF}}$, and the concentration of yeast in the feed, $c_{\text{yeast,Feed}}$ (Eq. (3)).

$$CR = \frac{c_{\text{yeast,UF}}}{c_{\text{yeast,Feed}}} \quad (3)$$

It was found that for the range of values investigated in the CCRD, the effect of changes in the vortex finder height on concentration ratio were not statistically significant. However, there was an effect on recovery, so the vortex finder height can be manipulated to enhance recovery without affecting the concentration ratio. The contour diagram of concentration ratio as a function of vortex finder and spigot diameters is presented in Fig. 4. It is observed that the concentration ratio can be increased by decreasing the diameter of the spigot, which can be linked to higher pressures that would be expected due to the

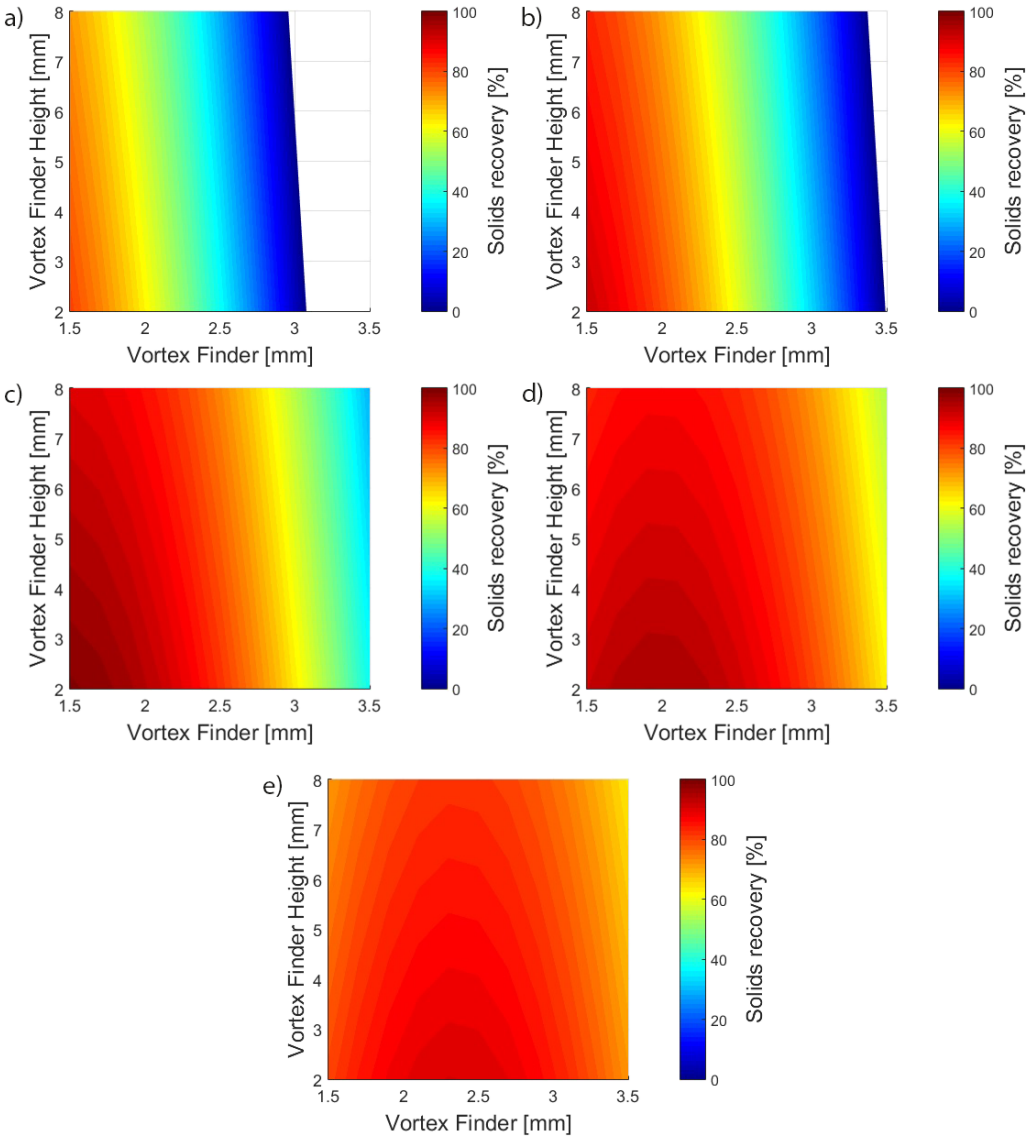

Figure 2. Contour diagrams of solids recovery as a function of vortex finder height and vortex finder diameter for different spigot diameters: (a) 1.5 mm, (b) 1.9 mm, (c) 2.5 mm, (d) 3.1 mm, (e) 3.5 mm.

reduction of the outlet diameter. The dependency of concentration ratio on vortex finder diameter, on the other hand, was found to be nonlinear.

As in the previous section, a regression analysis provided the model for the concentration ratio as indicated in Eq. (4). The model, which has a coefficient of determination of $R^2 = 0.921$, includes all predictors for which p values were lower than 0.05. Eq. (4) is shown without the regression coefficients, which are reported in Tab. 5.

$$CR = 1 + VF + SP + VF\,SP + VF^2 \quad (4)$$

Table 5. Regression coefficients for the concentration ratio model. Values for the statistically significant design variables (p value < 0.05) are presented; $R^2 = 0.921$.

	Regression coefficient
Intercept	1.3264
VF	0.9952
SP	–0.74592
VF/SP	0.17267
VF^2	–0.26409

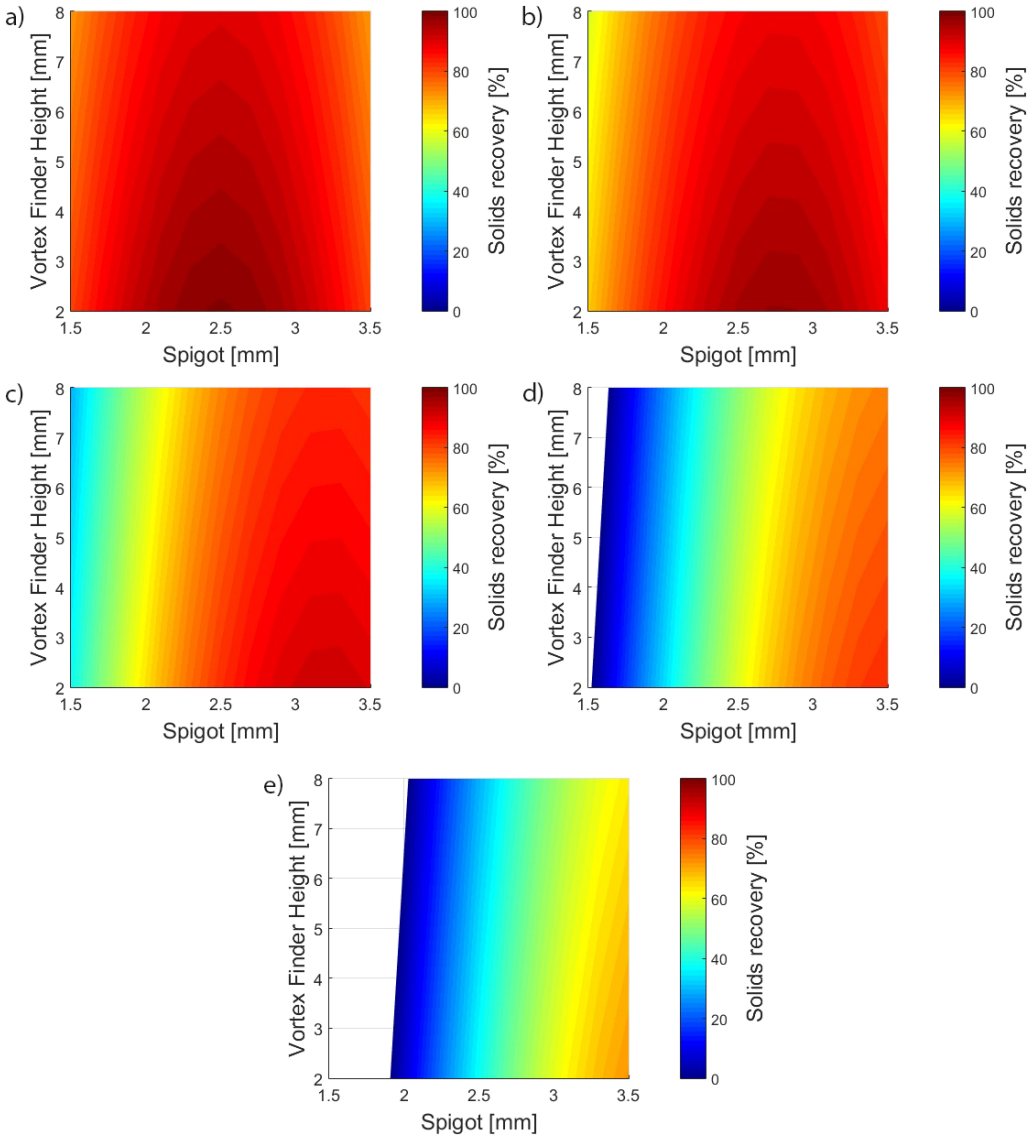

Figure 3. Contour diagrams of solids recovery as a function of vortex finder height and spigot diameter for different vortex finder diameters: (a) 1.5 mm, (b) 1.9 mm, (c) 2.5 mm, (d) 3.1 mm, (e) 3.5 mm.

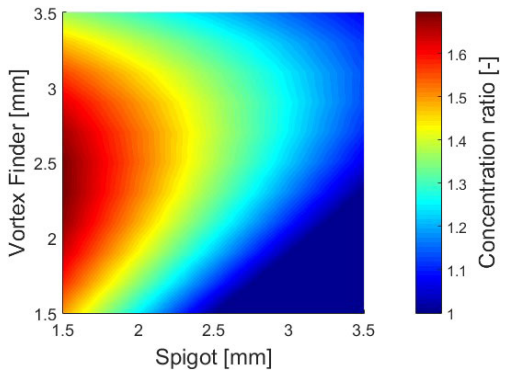

Figure 4. Contour diagram of concentration ratio as a function of vortex finder and spigot diameters. The vortex finder height was found to have no effect on the concentration ratio.

3.3 Selection of an Optimal Mini-hydrocyclone Design

The mathematical models obtained for the recovery of yeast and concentration ratio in the mini-hydrocyclones can be used to inform on the selection of optimal design parameters. For these separation units, however, performance is a trade-off between recovery and concentration ratio, and the optimal design will be governed by the specific requirements of the operation, which is often dependent on further downstream processing.

A recovery-concentration ratio curve can be useful to assess the performance of a given mini-hydrocyclone unit with respect to other designs. Moreover, based on the models in Eqs. (2) and (4), and constraining the ranges of values of the design variables to those tested on the CCRD, a Pareto front can be

obtained that shows the maximum recovery which can be attained for a given concentration ratio, or vice versa. Fig. 5 displays such a Pareto front, while some of the designs that sit on the Pareto front are included in Tab. 6. This procedure can help in the selection of a mini-hydrocyclone design for either the dewatering of yeast suspensions or the recovery of yeast cells.

Table 6. Mini-hydrocyclone design parameters obtained by maximizing recovery in the surface response models at various values of concentration ratio, or vice versa.

VF [mm]	*SP* [mm]	*VF-H* [mm]	*R* [%]	*CR* [–]
1.72	2.34	2	96.27	1.2
1.78	2.18	2	92.82	1.3
1.77	1.94	2	87.48	1.4
1.71	1.67	2	80	1.5
1.79	1.5	2	71	1.6
2.37	1.5	2	44.6	1.7

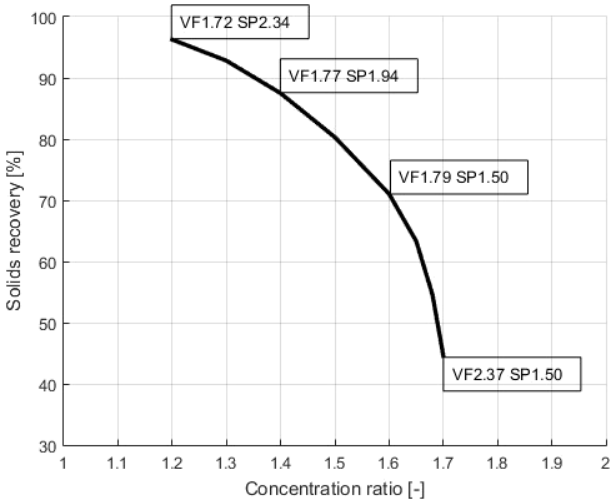

Figure 5. Recovery-concentration ratio curve showing the Pareto front for mini-hydrocyclone performance. This shows the trade-off between recovery and concentration ratio and can be useful for the selection of an optimal mini-hydrocyclone design for a particular process. Selected designs are indicated on the Pareto front, with their corresponding values of vortex finder (*VF*) and spigot (*SP*) diameters.

4 Conclusions

A CCRD study has been conducted to understand the effect that mini-hydrocyclone design parameters have on the separation performance of yeast suspensions. 3D printing was used to manufacture the mini-hydrocyclones with different spigot diameters, vortex finder heights, and vortex finder diameters. By means of this 3D printing technology, it was possible to accurately control the aforementioned design parameters, which had in the past been a limitation to study designs other than those of commercially available mini-hydrocyclones.

The experimental design allowed the assessment of the impact that these variables have on the recovery of yeast and the concentration ratio. It was found that recovery is affected by all the design variables, including nonlinear effects for the spigot and vortex finder diameters. The concentration ratio was found not to be influenced by the height of the vortex finder, which indicates that this design variable can be adjusted to optimize recovery without compromising the concentration ratios that can be achieved.

Mathematical models were obtained from regression analyses that included the interactive effect of the predictors as well as second-order terms. The models were applied to find optimal mini-hydrocyclone designs that maximize separation performance, for which the trade-off between recovery and concentration ratio had to be considered. A Pareto front was generated that can be used to inform on the selection of optimal mini-hydrocyclone design parameters for a particular process.

Acknowledgment

This research received funding from the European Union's (EU's) framework program for research and innovation Horizon 2020 (2014–2020) under grant agreement no. 637077 (project PRODIAS). The authors would like to thank Mr. Francisco Reyes for valuable discussions.

The authors have declared no conflict of interest.

Symbols used

$c_{yeast,Feed}$	[g L^{-1}]	concentration of yeast in the feed
$c_{yeast,UF}$	[g L^{-1}]	concentration of yeast in the underflow
CR	[–]	concentration ratio
d	[µm]	particle diameter
$m_{yeast,Feed}$	[mL s^{-1}]	mass flow rate of particles (yeast) in the feed
$m_{yeast,UF}$	[mL s–]	mass flow rate of particles (yeast) in the underflow
R	[%]	recovery of solids
R^2	[–]	coefficient of determination
SP	[mm]	spigot diameter
VF	[mm]	vortex finder diameter
VF-H	[mm]	vortex finder height

Abbreviation

CCRD	central composite rotatable design

References

[1] H.-J. Henzler, *Chem. Ing. Tech.* **2012**, *84 (9)*, 1482–1496. DOI: https://doi.org/10.1002/cite.201200003

[2] R. C. V. Pinto, R. A. Medronho, L. R. Castilho, *Cytotechnology* **2008**, *56 (1)*, 57–67. DOI: https://doi.org/10.1007/s10616-007-9108-x

[3] M. Habibian, M. Pazouki, H. Ghanaie, K. Abbaspour-Sani, *Chem. Eng. J.* **2008**, *138 (1–3)*, 30–34. DOI: https://doi.org/10.1016/j.cej.2007.05.025
[4] J. J. Cilliers, S. T. L. Harrison, *Chem. Eng. J.* **1997**, *65 (1)*, 21–26. DOI: https://doi.org/10.1016/S1385-8947(96)03100-2
[5] I. C. Bicalho, J. L. Mognon, J. Shimoyama, C. H. Ataíde, C. R. Duarte, *Sep. Sci. Technol.* **2013**, *48 (6)*, 915–922. DOI: https://doi.org/10.1080/01496395.2012.712597
[6] J. J. Cillliers, S. T. L. Harrison, *Sep. Purif. Technol.* **2019**, *209*, 159–163. DOI: https://doi.org/10.1016/j.seppur.2018.06.019
[7] I. C. Bicalho, J. L. Mognon, J. Shimoyama, C. H. Ataíde, C. R. Duarte, *Sep. Purif. Technol.* **2012**, *87*, 62–70. DOI: https://doi.org/10.1016/j.seppur.2011.11.023
[8] A. A. Pinto, I. C. Bicalho, J. L. Mognon, C. R. Duarte, C. H. Ataíde, *Sep. Purif. Technol.* **2013**, *120*, 69–77. DOI: https://doi.org/10.1016/j.seppur.2013.09.013
[9] F. He, Y. Zhang, J. Wang, Q. Yang, H. Wang, Y. Tan, *Chem. Eng. Technol.* **2013**, *36 (11)*, 1935–1942. DOI: https://doi.org/10.1002/ceat.201300204
[10] K.-J. Hwang, S.-P. Chou, *Sep. Purif. Technol.* **2017**, *172*, 76–84. DOI: https://doi.org/10.1016/j.seppur.2016.08.005
[11] D. Vega-Garcia, P. R. Brito-Parada, J. J. Cilliers, *Chem. Eng. J.* **2018**, *350*, 653–659. DOI: https://doi.org/10.1016/j.cej.2018.06.016
[12] M. Shakeel Syed, M. Rafeie, R. Henderson, D. Vandamme, M. Asadnia, M. Ebrahimi Warkiani, *Lab Chip* **2017**, *17 (14)*, 2459–2469. DOI: https://doi.org/10.1039/c7lc00294g
[13] J. J. Cilliers, R. C. Austin, J. P. Tucker, in *Hydrocyclones: Analysis and Applications* (Eds: L. Svarovsky, M. T. Thew), Fluids Mechanics and its Applications, Vol. 12, Springer, Dordrecht **1992**, 31–49. DOI: https://doi.org/10.1007/978-94-015-7981-0_3

